Since January 2020 Elsevier has created a COVID-19 resource centre with free information in English and Mandarin on the novel coronavirus COVID-19. The COVID-19 resource centre is hosted on Elsevier Connect, the company's public news and information website.

Talanta 79 (2009) 295–301

Contents lists available at ScienceDirect

Talanta

journal homepage: www.elsevier.com/locate/talanta

A self-assembled fusion protein-based surface plasmon resonance biosensor for rapid diagnosis of severe acute respiratory syndrome

Tae Jung Park[a], Moon Seop Hyun[b], Hye Jin Lee[c], Sang Yup Lee[a,d], Sungho Ko[e,*]

[a] BioProcess Engineering Research Center, Center for Systems & Synthetic Biotechnology, Institute for the BioCentury, KAIST, 335 Gwahangno, Yuseong-gu, Daejeon 305-701, Republic of Korea
[b] National NanoFab Center, 335 Gwahangno, Yuseong-gu, Daejeon 305-806, Republic of Korea
[c] Department of Chemistry, Kyungpook National University, 1370 Sankyuk-dong, Buk-gu, Daegu 702-701, Republic of Korea
[d] Department of Chemical & Biomolecular Engineering (BK21 program), Department of Bio & Brain Engineering, Department of Biological Sciences, Bioinformatics Research Center, KAIST, 335 Gwahangno, Yuseong-gu, Daejeon 305-701, Republic of Korea
[e] Korea Food Research Institute, 516 Baekhyun-dong, Bundang-gu, Seongnam 463-746, Republic of Korea

ARTICLE INFO

Article history:
Received 29 December 2008
Received in revised form 20 March 2009
Accepted 23 March 2009
Available online 1 April 2009

Keywords:
Surface plasmon resonance
Biosensor
Severe acute respiratory syndrome
Fusion protein
Gold binding polypeptide

ABSTRACT

A surface plasmon resonance (SPR)-based biosensor was developed for simple diagnosis of severe acute respiratory syndrome (SARS) using a protein created by genetically fusing gold binding polypeptides (GBPs) to a SARS coronaviral surface antigen (SCVme). The GBP domain of the fusion protein serves as an anchoring component onto the gold surface, exploiting the gold binding affinity of the domain, whereas the SCVme domain is a recognition element for anti-SCVme antibody, the target analyte in this study. SPR analysis indicated the fusion protein simply and strongly self-immobilized onto the gold surface, through GBP, without surface chemical modification, offering a stable and specific sensing platform for anti-SCVme detection. AFM and SPR imaging analyses demonstrated that anti-SCVme specifically bound to the fusion protein immobilized onto the gold-micropatterned chip, implying that appropriate orientation of bound fusion protein by GBP resulted in optimal exposure of the SCVme domain to the assay solution, resulting in efficient capture of anti-SCVme antibody. The best packing density of the fusion protein onto the SPR chip was achieved at the concentration of 10 $\mu g\,mL^{-1}$; this density showed the highest detection response (906 RU) for anti-SCVme. The fusion protein-coated SPR chip at the best packing density had a lower limit of detection of 200 $ng\,mL^{-1}$ anti-SCVme within 10 min and also allowed selective detection of anti-SCVme with significantly low responses for non-specific mouse IgG at all tested concentrations. The fusion protein provides a simple and effective method for construction of SPR sensing platforms permitting sensitive and selective detection of anti-SCVme antibody.

1. Introduction

Severe acute respiratory syndrome (SARS) is a newly emerged disease of global significance because of its highly contagious nature. Extensive human worldwide travel, and contact with animals [1,2], contribute to the SARS problem. Early detection and identification of SARS coronavirus (CoV)-infected patients, and actions to prevent transmission, are absolutely critical in prevention of another SARS outbreak [1,3]. Although enzyme-linked immunosorbent assays (ELISAs) and real-time PCR-based diagnostic tests for SARS have been valuable for early identification of infections, they are still laborious and expensive and require skilled personnel [3–5]. Therefore, in terms of public health measures in response to epidemics, a rapid recognition of emerging SARS infections urgently requires new diagnostic tools that are portable, sensitive, and easy to use, to assure (as much as possible) "in-field" detection.

Recently, surface plasmon resonance (SPR)-based biosensors have been developed for the direct monitoring of antigen–antibody interactions. Such sensors offer several advantages: there is no need for labeling; real-time detection is possible; curtailment of non-specific binding is achievable; and detection of nanomolar concentrations of proteins of molecular weights larger than 180 Da is possible [6,7]. In principle, a surface plasmon oscillation is a localized wave that propagates along the interface between the gold film and the ambient medium and is very sensitive to changes in the refractive index near the gold surface when biomolecules bind to that surface [7,8].

One of the main issues in the development of biosensors is efficient immobilization of biomolecules on the sensor surface. Many protein immobilization techniques, based on both physical adsorption and covalent linkage, have been developed in the past few

* Corresponding author. Tel.: +82 31 780 9320; fax: +82 31 780 9228.
E-mail address: shko7@kfri.re.kr (S. Ko).

0039-9140/$ – see front matter © 2009 Elsevier B.V. All rights reserved.
doi:10.1016/j.talanta.2009.03.051

years [9]. However, the physical attachment to surface is likely to be heterogeneous, weak, and randomly oriented, and the covalent attachment also can lead to random immobilization of proteins, resulting in a reduction of biological activity. Such techniques are cumbersome and time-consuming. Therefore, a simple method to immobilize target proteins, with retention of biological activity, is urgently required.

A gold binding polypeptide (GBP) containing triple repeats of a particular 14 amino acid sequence is able to bind metallic gold [10]. Interestingly, none of these 14 amino acid residues is cysteine, generally considered to form a thiol linkage with gold [11], thus offering a new way of interaction between proteins and gold surfaces. Polar side-chains of peptides rich in serine and threonine seem to interact with the gold surface. The adsorption kinetics of GBP onto the gold surface were explored using SPR spectroscopy [12]. Furthermore, proteins and peptides of interest can be fused to the GBP for immobilization on the gold surface [13]. These findings led us to develop protein immobilizations of biological sensors using GBP as a fusion partner.

In this paper, we developed a simple protein immobilization method employing genetically engineered GBP-fused proteins as both biolinkers and ligands, to create a SARS diagnosis technique employing an SPR detection system. The GBP-fusion proteins consist of two domains of the GBP fused to SARS-CoV membrane-envelope (SCVme) protein. The fusion proteins can be directly self-assembled onto the SPR gold surfaces via the GBP portions without complicated chemical modification of the gold surface, and the SCVme portion serves as a capture ligand for anti-SCVme antibody.

2. Experimental

2.1. Chemicals and reagents

Unless otherwise stated, all chemical reagents were purchased from Sigma–Aldrich (St. Louis, MO, USA). Rabbit anti-SCVme polyclonal antibody was prepared by immunization with a peptide corresponding to residues 58–75 (COOH-CVYSRVKNLNSSEGVPDLL-NH_2) of the envelope protein, according to the manufacturer's procedures (Peptron, Daejeon, Korea). All restriction enzymes were purchased from New England Biolabs (Beverly, MA, USA). Phosphate-buffered saline (PBS, pH 7.4) from BD Biosciences (San Jose, CA, USA) was used as a flow solution and dilution buffer for SPR analysis. Distilled water (18 MΩ cm) was obtained using an ultrapure water system (Milli-Q; Millipore, Billerica, MA, USA).

2.2. Preparation of SARS-CoV envelope gene

Antigenic regions were predicted by analyzing the primary structure of the SARS-CoV envelope protein. Oligonucleotides encoding the SARS-CoV envelope protein were synthesized by design of gene sequence from the envelope amino acid sequence, employing the DNAWorks program [14]. The sequence encoding the SARS-CoV envelope protein was obtained from GenBank (accession number AY274119.3). The relevant gene was located from base pairs 26,117–26,347 in the SARS genomic sequence, and encoded 76 amino acids [1]. The codon frequency was chosen to represent *Escherichia coli* class II, and the following parameters were employed: maximum oligonucleotide length, 50 nt; annealing temperature, 58 °C; codon frequency threshold, 50; number of solutions, 50. Synthetic assembly of the intact envelope gene using component oligonucleotides was performed with a single-step assembly protocol [15]. We describe the approach only in general. Polymerase chain reaction (PCR) experiments for gene assembly were carried out under the following cycling conditions: initial denaturing step at 94 °C for 5 min to avoid any possible mispriming; 30 cycles of denaturing at 94 °C for 30 s; annealing at various temperatures (depending on the melting temperatures indicated by the DNAWorks program); extension at 72 °C for 1 min; and a final extension at 72 °C for 7 min. For gene amplification, 1 μL of the mixture from the gene assembly reaction was used as a template, with the outermost oligonucleotides used as primers. As in a previous report [2], PCR experiments were performed using a Thermal Cycler (Bio-Rad, Hercules, CA, USA) and high-fidelity Taq polymerase (Takara Bio, Shiga, Japan) for the cloning of the SARS-CoV envelope gene in *E. coli*. All DNA manipulations including restriction digestion, ligation, and agarose gel electrophoresis, were standard procedures [16]. The DNA sequence of the clone was confirmed by automatic DNA sequencing (ABI Prism 377, PerkinElmer, Grove, IL, USA).

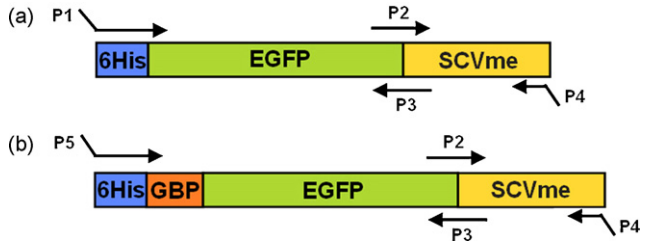

Fig. 1. Synthesis of (a) E-SCVme and (b) GBP-E-SCVme fusion genes by overlap PCR. Abbreviations are: 6His, six histidines; EGFP, enhanced green fluorescent protein; GBP, gold binding polypeptide; SCVme, the SARS-CoV membrane-envelope chimera protein.

2.3. Preparation of GBP-EGFP-SCVme fusion proteins

Bifunctional fusion proteins were created by genetically fusing GBP and SCVme to enhanced green fluorescent protein (EGFP), allowing for two specific interactions between GBP and gold substrates, and the capture of SCVme and anti-SCVme antibodies by SCVme. EGFP from the jellyfish *Aequorea victoria* was used as a model protein for soluble expression of the fusion proteins and offered convenient monitoring of soluble fractions, and a six-histidine (6His) was tagged to easily purify the fusion proteins. The DNA fragment encoding 6His-EGFP was first amplified by PCR with the primers P1 (5′-GCGAATTCCATGGTGCACCATCACCATCACCATAGCAAGGGCGAGGAG-3′) and P3 (5′-ACAAAAACCTGTTCCGATTCTTGTACAGCTCGTCCATGCC-3′), using the plasmid pEGFP (BD Biosciences) as a template. Then, the fusion of the DNA fragment encoding incomplete SCVme to 6His-EGFP was achieved by PCR amplification with the primers P2 (5′-GGCATGGACGAGCTGTACAAGAATCGGAACAGGTTTTTGT-3′) and P4 (5′-CGGAATTCAAGCTTTTAGACCAGAAGATCAGGAAC-3′), using pTrc-6HSCVme::AfBD [2] as a template. Finally, the complete 6His-EGFP-SCVme (E-SCVme) fusion gene fragment was amplified with the primers P1 and P4 using the PCR products encoding 6His-EGFP and SCVme as templates (Fig. 1(a)). The PCR product was digested with NcoI and HindIII, and ligated into the NcoI–HindIII fragment of pTrc99A (GE Healthcare, Piscataway, NJ, USA) to construct pTESCVme expressing E-SCVme fusion protein.

For the cloning of 6His-GBP-EGFP-SCVme (GBP-E-SCVme) fusion gene (Fig. 1(b)), DNA fragments encoding EGFP and the SCVme fusion gene were amplified by PCR as previously reported [2]. The DNA fragment encoding 6His-GBP-EGFP was first amplified by PCR with the primers P3 and P5 (5′-GCGAATTCCATGGGC-*CACCATCACCATCACCAT*GGCAAAACCCAGGCGACCA-3′) using the plasmid pTGE as a template. A DNA fragment encoding SCVme was amplified using primers P2 and P4. Finally, the GBP-E-SCVme fusion gene was amplified with primers P4 and P5 using the above PCR products as templates. The amplified GBP-E-SCVme

fusion gene was digested with NcoI and HindIII, and ligated into the NcoI–HindIII fragment of pTrc99A to construct pTGESCVme expressing GBP-E-SCVme fusion protein.

For expression of the fusion proteins, plasmids were consecutively introduced into *E. coli* XL1-Blue strain (*recA1*, *endA1*, *gyrA96*, *thi*, *hsdR17*, *suppE44*, *relA1*, l^-, *lac*$^-$, F′[*proAB lacI*^{q} lacZΔM15, Tn*10* (tet)^r]), from Stratagene, La Jolla, CA, USA using a Gene Pulser electroporator (Bio-Rad) in accordance with the manufacturer's instructions. The *E. coli* transformants harboring pTESCVme and pTGESCVme were cultivated in Luria–Bertani (LB) medium (tryptone 10 g L^{-1}, yeast extract 5 g L^{-1}, NaCl 5 g L^{-1}) with ampicillin (100 μg mL^{-1}) at 37 °C in a shaking incubator (200 rpm). Cell growth was monitored by measuring optical density at 600 nm (OD_{600}) using a spectrophotometer (DU®650, Beckman, Fullerton, CA, USA). When cultures reached OD_{600} values of 0.6, the expression of the *trc* promoter was induced by adding 1 mM (final concentration) isopropyl-β-D-thiogalactopyranoside (IPTG) to culture broth. After further cultivation for 6 h, cells were harvested by centrifugation at 10,000 × *g* for 10 min at 4 °C and disrupted by sonication (Braun Ultrasonics, Danbury, CT, USA) for 1 min at 40% of output power. After centrifugation at 16,000 × *g* for 10 min at 4 °C, the supernatant containing soluble proteins was obtained for further analysis. Because of the 6His tags, the E-SCVme and GBP-E-SCVme fusion proteins were simply purified using Ni-chelating resin (Qiagen, Valencia, CA, USA).

2.4. Fabrication of gold micropatterns

To prepare gold-patterned chips, glass slides were washed with piranha solution (75% H_2SO_4/25% H_2O_2, v/v) to enhance gold adhesion onto the glass substrate. An AZ9260 positive photoresist (SU-8, Microchem, Newton, MA, USA) master was made on the slide by even pouring and spin-coating at 2000 rpm for 60 s. To remove volatile organics, the slide was cured in a convection oven at 110 °C for 3 min. After slow cooling, the slide was exposed to ultraviolet (UV) light for 75 s at a temperature below 30 °C, which was very useful to prevent the photoresist cracking. UV-exposed slides were then treated with AZ9260 developer for about 5 min, and then UV-exposed photoresist was removed, but SU-8-negative photoresist was retained. A thermal evaporation unit was used to deposit the chromium and gold onto the slide glass, in which height was controlled to be 5 and 40 nm, sequentially. Following gold deposition, the slides were soaked in acetone to remove the AZ9260 photoresist over 4 h. Finally, the gold patterns of 50-μm circle in diameter remained only on the developed region, where no photoresist existed after development.

2.5. Atomic force microscopy (AFM) imaging analysis

The GBP-E-SCVme fusion protein was immobilized onto the gold-micropatterned substrate by dipping the substrate into a solution of GBP-E-SCVme (100 μg mL^{-1}) for 30 min at 25 °C, followed by washing with distilled water and drying with nitrogen gas. Anti-SCVme antibodies (100 μg mL^{-1}) were sequentially treated onto the substrate surface by dipping in antibody solution for 30 min at 25 °C. Following washing and drying of the prepared chip, the surface morphology and the height of each layer formed were investigated by AFM. The AFM analyses were performed using an XE-100 Scanning Probe Microscope system (Park Systems, Suwon, Korea) in the non-contact mode, employing a Tap300Al cantilever (Budget Sensors, Sofia, Bulgaria) with an aluminum reflex coating on the reverse side of the cantilever. The spring constant and the resonance frequency of the cantilever were typically 40 N m^{-1} and 300 kHz, respectively. The AFM images of the gold micropatterns were acquired in an ambient atmosphere (40–50% relative humidity) at a speed of 1.0 Hz and a resolution of 512 × 512 pixel. To analyze surface roughness, and to verify the height of each layer on the surface of glass slides, sample surfaces were scanned in an AFM feedback loop in a manner permitting changes in cantilever vibrational amplitude to be recorded. Feedback signals were used to generate a topographic image. The phase lag was monitored while each topographic image was being taken so that several topographic images could be simultaneously collected.

2.6. Binding properties of GBP-E-SCVme fusion proteins onto SPR chip surfaces

The binding of GBP-E-SCVme fusion protein onto the surface of the SPR bare gold chip was characterized by SPR measurement using a BIAcore3000™ instrument (Biacore AB, Uppsala, Sweden) with an automatic flow injection system. A fresh SPR sensor chip was attached to a separate chip carrier for easy assembly in the SPR system. After the SPR chip was docked and primed, PBS was used to flush the activated surface, to minimize non-specific binding and any unbound sites by removing loosely bound material and dust. Fifty microliters of GBP-E-SCVme fusion protein (0.1 mg mL^{-1}) or E-SCVme fusion protein (negative control, 0.1 mg mL^{-1}) were injected onto the chip surface for 10 min using a liquid-handling micropipette in the SPR system, and the surface was then washed and equilibrated with PBS. The SPR responses are indicated in resonance units (RUs). All SPR experiments in this study were conducted in PBS at a flow rate of 5 μL min^{-1} at 25 °C, and all sensorgrams were fitted globally using BIA evaluation software.

2.7. Sensitivity and selectivity of the GBP-E-SCVme-coated SPR biosensor

To examine the sensitivity of the GBP-E-SCVme-coated SPR chip, various anti-SCVme antibody concentrations (0.1, 0.2, 1, 10, 50, and 100 μg mL^{-1}) were applied to the chip surface covered with the GBP-E-SCVme, at optimal packing density determined above, for 10 min after blocking of non-specific binding with BSA for 10 min. Then, the chip was rinsed with PBS. The limit of detection (LOD) was determined by measuring the lowest anti-SCVme concentration showing a significant change in signal over the baseline obtained with the PBS. As tests for selective detection, solutions of 1 and 10 μg mL^{-1} of mouse IgG (negative controls) were allowed to flow over fresh SPR chips coated with GBP-E-SCVme, at the optimal packaging density, for 10 min,

2.8. SPR imaging (SPRi) analysis

The gold-micropatterned chip was loaded onto an SPRi apparatus (SPR*i*, K-MAC, Daejeon, Korea) using an incoherent light source (a 150 W quartz tungsten-halogen lamp; Schott, Mainz, Germany) for excitation. Briefly, ρ-polarized collimated white incident light on a prism/gold/thin film/buffer flow cell assembly was set at a fixed incident angle. Reflected light from this assembly was passed via a bandpass filter centered at a wavelength of 830 nm and collected by a CCD camera (Sony, Tokyo, Japan). Data images were collected digitally via a B/W frame grabber. Scion Image release Beta 4.0.3 software (Scion Corp., Frederick, MD, USA) was used to analyze the images.

3. Results and discussion

3.1. Surface morphology for binding of GBP-E-SCVme and anti-SCVme onto the gold surface

Fabrication processes for homogeneous stable monolayer structures have been developed to control the surface orientations

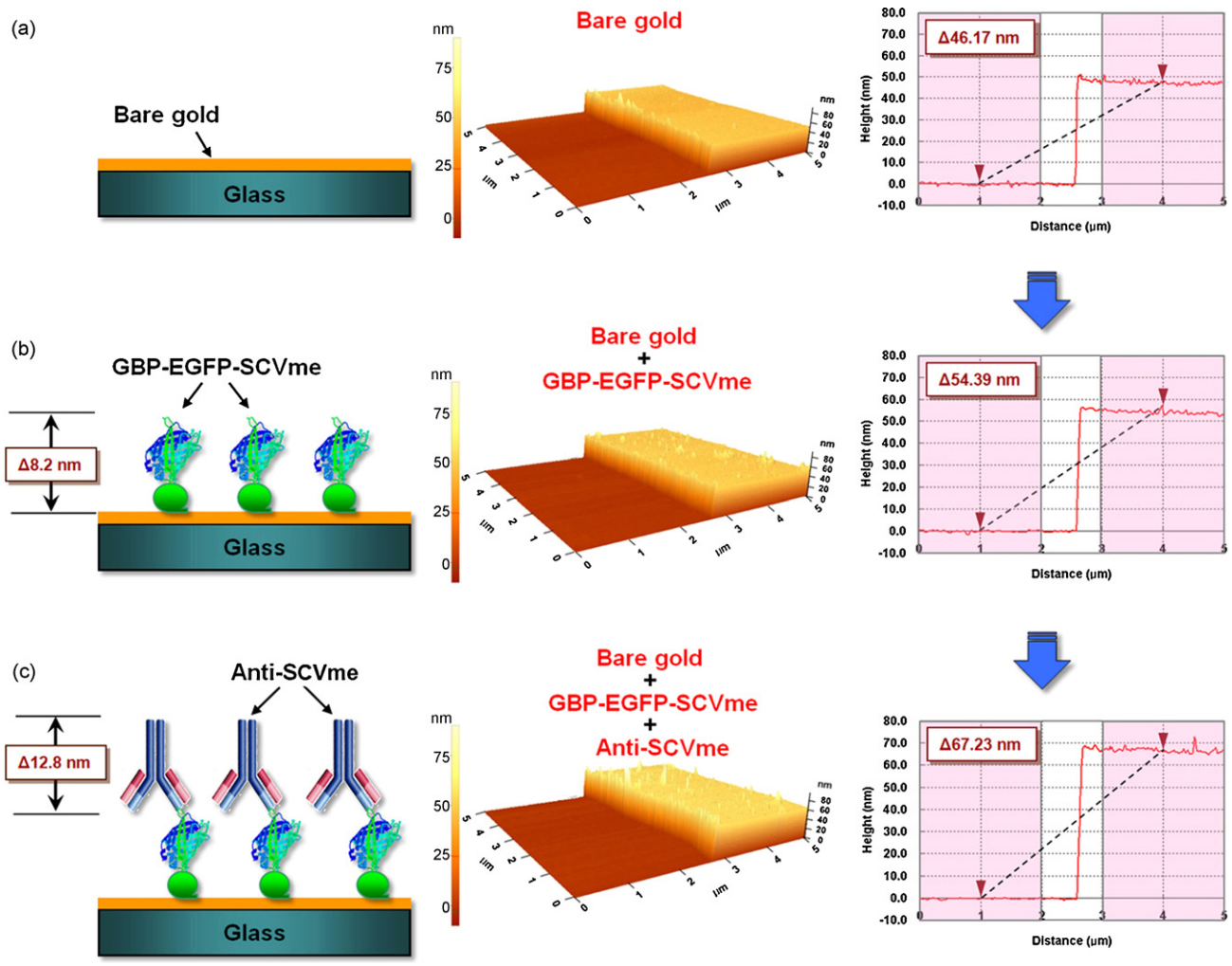

Fig. 2. AFM images of the sequential binding of GBP-E-SCVme and anti-SCVme on the gold-micropatterned surface. (a) Bare gold surface, (b) binding of the GBP-E-SCVme fusion proteins onto the gold surface, and (c) subsequent binding of the anti-SCVme antibodies on the GBP-E-SCVme layer. Left, schematic diagrams for the successive binding of GBP-E-SCVme and anti-SCVme on the gold micropatterns; middle, three-dimensional topological images; right, the cross-sectional contours of samples a–c, sequentially (these are average height differences of the individual scan lines from each area).

of biomolecules [17,18]. However, such fabrications require surface chemical modifications involving reactive functional groups or charged materials. Uniformly oriented immobilization of the GBP-E-SCVme fusion protein onto the gold chip was easily achieved without any surface chemical modification because of the gold binding property of the protein. To examine whether protein monolayers and protein molecular interactions might develop on the gold chip surface, we analyzed, at the molecular level, alterations in surface morphologies caused by sequential binding of GBP-E-SCVme and anti-SCVme antibodies onto a gold surface, employing high-resolution AFM analysis. After the specific immobilization of the GBP-E-SCVme ($100\,\mu g\,mL^{-1}$) onto the gold-micropatterned surface, the subsequent binding of anti-SCVme antibodies ($100\,\mu g\,mL^{-1}$) onto the GBP-E-SCVme layer was observed (Fig. 2). GFP has a 4.2 nm long cylindrical structure with a MW of ~27 kDa [19]. As GBP-E-SCVme fusion protein has a MW of ~57 kDa, the length of GBP-E-SCVme can be estimated to be ~8.87 nm. The line profile of the GBP-E-SCVme bound onto the micropatterned gold surface was measured as approximately 8.2 nm as a height difference from the gold surface (Fig. 2(a) and (b)). The height difference after binding with anti-SCVme antibodies was about 12.8 nm, which shows specific interaction of antibodies with the monolayer of GBP-E-SCVme immobilized onto the gold substrate (Fig. 2(b) and (c)). Furthermore, roughness increases caused by sequential binding of GBP-E-SCVme and anti-SCVme onto the gold surface were observed with different surface properties. Three-dimensional images show distinct well-shaped and well-defined peaks on the gold surface, and the gradual rise in peak numbers of Fig. 3(b) and (c) also indicates an increase in binding of biomolecules, suggesting that the GBP-E-SCVme and anti-SCVme antibodies were sequentially and specifically immobilized on the gold surface as ordered monolayers with a uniform thickness.

3.2. SPR analysis of GBP-fusion protein binding

The binding properties of the GBP-E-SCVme onto the gold surface were examined as shown in Fig. 3. The dynamic and specific binding of GBP-E-SCVme onto the SPR gold chip was directly monitored in real-time. A sharp increase in the SPR signal up to about 3060 RU was observed upon introducing GBP-E-SCVme solution onto the chip surface, and about 98% of the GBP-E-SCVme remained to the surface even after washing with PBS, which showed that most of the fusion protein was strongly immobilized onto the chip surface. The 3000 RU value obtained implies that about 3 ng of GBP-E-SCVme was immobilized onto a gold surface area of 1 mm^2. One RU is determined as 0.0001° of resonance angle shift and equivalent to a mass change of the $1\,pg\,mm^{-2}$ on the sensor surface [20,21]. However, the SPR signal of 3057 RU generated from the binding of

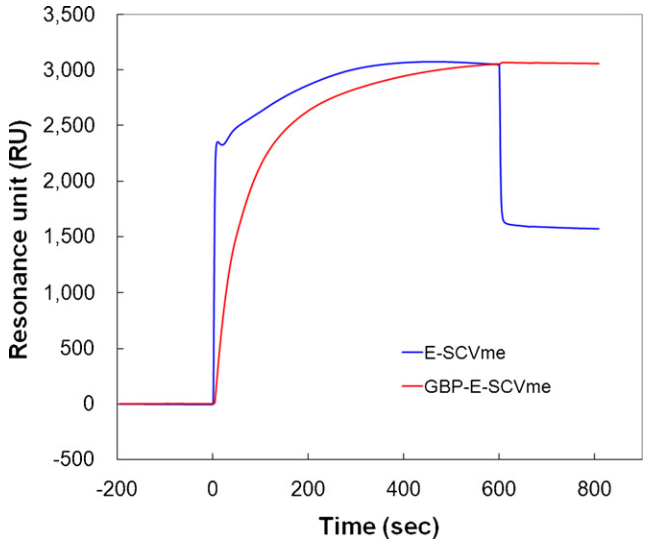

Fig. 3. SPR sensorgrams showing the specific immobilization of GBP-E-SCVme fusion proteins onto the gold chip. Red line, GBP-E-SCVme of 100 μg mL^{-1} (3057 RU); blue line, E-SCVme of 100 μg mL^{-1} (1574 RU) as a negative control. (For interpretation of the references to color in this figure legend, the reader is referred to the web version of the article.)

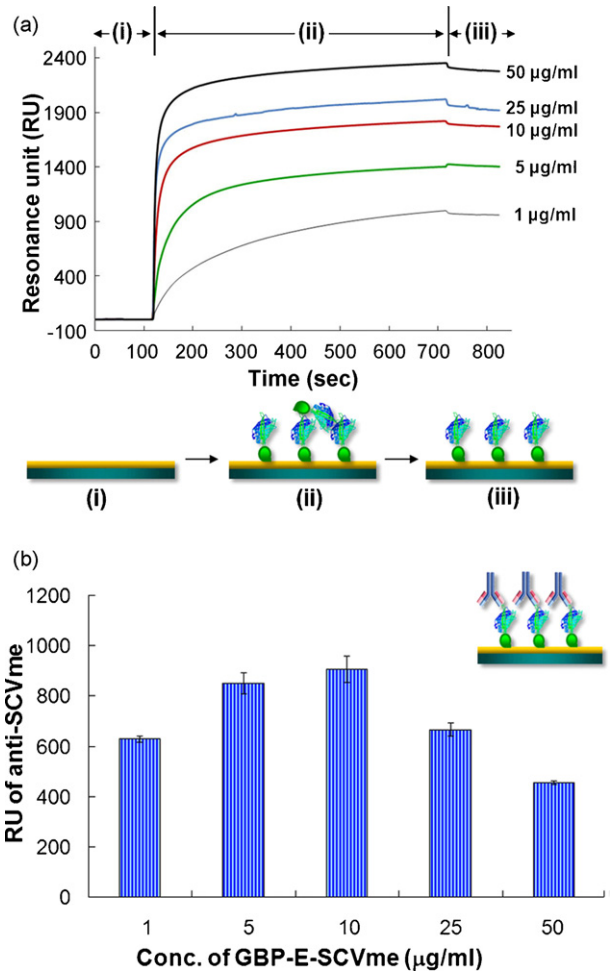

Fig. 4. (a) SPR sensorgrams showing the specific immobilization of GBP-E-SCVme fusion proteins onto the gold chip at various concentrations (1, 5, 10, 25, and 50 μg mL^{-1}). Each SPR phase was explored: (i) before immobilization, (ii) after binding of GBP-E-SCVme fusion proteins, and (iii) after washing with PBS. (b) Optimal concentration of GBP-E-SCVme immobilized onto the SPR gold chip, showing the highest signal from subsequent binding of anti-SCVme antibodies.

E-SCVme (control) onto the chip surface immediately decreased up to around 50% on rinsing with PBS, indicating that about 50% of E-SCVme was non-specifically bound to the gold surface. Positive surface charges of the amine groups in E-SCVme proteins may be irregularly coupled with negative charges of the gold surface by electrostatic force [22,23]. This showed that the electrostatic binding force was even weaker than the specific binding between GBP and the gold surface, and that GBP-E-SCVme fusion proteins could be strongly immobilized onto the gold surface by the GBP domain. Previous work also reported that the binding of GBP onto the gold surface is stronger than that of self-assembled monolayers of alkanethiol molecules due to the lower standard Gibbs free energy of GBP [12]. Therefore, it is clear that strong binding or adsorption of GBP-fusion protein onto the SPR chip can assist in studies on various protein–protein interactions.

3.3. *Optimal packing density of GBP-E-SCVme onto the gold surface*

In the study of the immunosensors, it is crucial to optimize the packing density of a recognition element immobilized onto a sensing surface in order to attain maximal sensitivity [24,25]. The amount of GBP-E-SCVme fusion protein immobilized onto the gold chip will affect the sensitivity of the SPR biosensor. To determine the optimal packing density, GBP-E-SCVme was immobilized onto the gold surface at various concentrations (1, 5, 10, 25, and 50 μg mL^{-1}), followed by washing out with PBS. Then, BSA (100 μg mL^{-1}) was injected onto the GBP-E-SCme-coated chips to block non-specific bindings. Finally, anti-SCVme antibody (100 μg mL^{-1}) was applied to the GBP-E-SCVme-layered surface in order to examine specific binding between GBP-E-SCVme and anti-SCVme by SPR biosensor response.

As shown in Fig. 4(a), the immobilization of GBP-E-SCVme onto the gold surface increased progressively from 950 to 2250 RU as GBP-E-SCVme concentration increased, indicating that GBP portion played an important role in surface self-immobilization of GBP-E-SCVme. Fig. 4(b) shows the interaction between the GBP-E-SCVme layer and subsequent applied anti-SCVme. When anti-SCVme was permitted to flow over the GBP-E-SCVme layer, SPR signals increased until the concentration of GBP-E-SCVme reached to 10 μg mL^{-1}, but they began to decrease as the concentration was over 10 μg mL^{-1}. Less than 10 μg mL^{-1}, 1 and 5 μg mL^{-1} concentrations of GBP-E-SCVme resulted in low levels of the fusion protein immobilized on the gold surface, resulting in insufficient interaction between GBP-E-SCVme and anti-SCVme. Moreover, lower signals of 680 and 480 RU compared to that (900 RU) observed at the concentration of 10 μg mL^{-1} GBP-E-SCVme were obtained at 25 and 50 μg mL^{-1} concentrations, respectively, because the GBP-E-SCVme was densely immobilized on the surface and thus steric hindrance between closely packed GBP-E-SCVme molecules may have occurred. These results indicate that the best packing density of GBP-E-SCVme was obtained using a 10 μg mL^{-1} solution concentration. This particular packing density of the GBP-E-SCVme likely reduced steric hindrance, provided sufficient binding sites for anti-SCVme antibody, and avoided loss of biological activity. Ko et al. [24,25] have shown similar trends that insufficiently or densely immobilized antibodies on sensing surfaces can lead to a reduced detection signal, and Kolotilov et al. [26] also showed that a nanoparticle with immobilized protein A could not anchor sufficient IgG molecules to its surface due to steric hindrances. The best packing density of GBP-E-SCVme determined here was used in subsequent experiments.

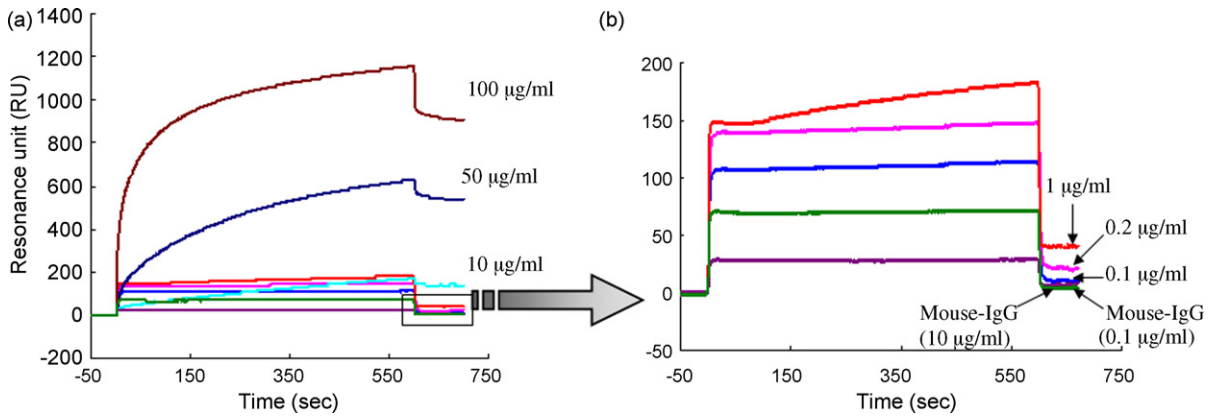

Fig. 5. SPR sensorgrams for (a) sensitive and (b) selective detection of anti-SCVme using the GBP-E-SCVme immobilized gold sensor chip at various concentrations (0.1, 1, 10, 50, and 100 μg mL^{-1}) of anti-SCVme and (1 and 10 μg mL^{-1}) of mouse IgG as negative controls.

3.4. Sensitivity and selectivity for SARS diagnosis

To investigate the sensitivity and selectivity of the SPR biosensor system using GBP-E-SCVme for detection of anti-SCVme antibody, the best concentration of GBP-E-SCVme (10 μg mL^{-1}) determined above was applied onto the gold surface to simply construct a sensitive SPR chip. The binding signal of anti-SCVme to the GBP-E-SCVme layer progressively increased from 11.3 to 905 RU as the anti-SCVme concentration increased from 0.1 to 100 μg mL^{-1}, respectively (Fig. 5(a)).

In addition, the selectivity of the GBP-E-SCVme-coated SPR sensor chip for detection of anti-SCVme was examined using mouse IgG (1 and 10 μg mL^{-1}) as negative controls (Fig. 5(b)). As expected, little SPR responses of 5.8 and 6.7 RU were observed by the non-specific binding of mouse IgG at 1 and 10 μg mL^{-1}, respectively. These SPR responses were much lower than those (43 and 142 RU) obtained when the anti-SCVme of 1 and 10 μg mL^{-1} concentrations, respectively, were used. Also, the slight difference between SPR signals of 5.8 and 6.7 RU means that the binding of mouse IgG was independent of concentration since it was only a negative control. It means that the GBP-E-SCVme-coated SPR chip selectively detects anti-SCVme antibodies.

Meanwhile, the lowest SPR response value (11.3 RU) by the binding of 0.1 μg mL^{-1} anti-SCVme among various concentrations was even differentiable from the control signal (6.7 RU) for 10 μg mL^{-1} of mouse IgG. However, low detection limit is normally the signal that is three times higher than the background signal [27,28]. The SPR signal of 25.2 RU at the anti-SCVme concentration of 0.2 μg mL^{-1} meets this requirement. Therefore, it was determined that the LOD of the GBP-E-SCVme immobilized sensor chip for detection of anti-SCVme in PBS was 0.2 μg mL^{-1}. It is considered that the best packing density of GBP-E-SCVme fusion proteins used in fabrication of the sensor chip may contribute to this low LOD. These results show that development of a sensitive and selective immunoassay system for SARS diagnosis was possible using a GBP-E-SCVme fusion protein-immobilized SPR chip.

3.5. SPRi analysis for detection of anti-SCVme antibodies on the gold micropatterns

After we determined that AFM imaging and SPR spectroscopy analyses could successfully be used to study biomolecular interactions on the gold surface, we visually confirmed the successive binding of GBP-E-SCVme and anti-SCVme antibodies onto the gold-micropatterned chip using an SPRi analysis system. The SPRi difference images produced by subtracting a reference image from a post-binding image contribute to visual confirmation of binding [29,30]. The gold-micropatterned chip was cleaned for 5 min in piranha solution and next washed with distilled water. After drying under nitrogen, the chip sequentially bound GBP-E-SCVme fusion proteins and anti-SCVme antibodies. The GBP-E-SCVme fusion proteins (from a 100 μg mL^{-1} solution) were immobilized onto the gold-micropatterned chip by dipping for 30 min at 25 °C. After the GBP-E-SCVme-treated chip was washed with distilled water and dried under nitrogen, the chip was dipped into a solution of anti-

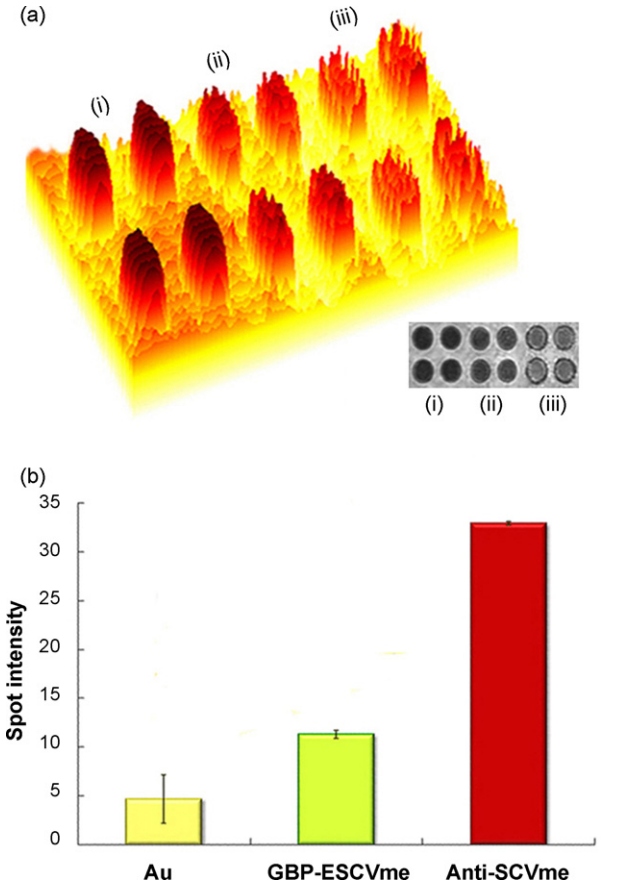

Fig. 6. SPRi analysis of the sequential binding of GBP-E-SCVme and anti-SCVme onto gold micropatterns composed of 50-μm diameter circles. (a) Three-dimensional and two-dimensional (inset) images of bare gold micropatterns as controls (sample (i)); binding of GBP-E-SCVme fusion proteins onto the gold patterns (sample (ii)); and successive binding of GBP-E-SCVme and anti-SCVme onto the gold patterns (sample (iii)). (b) Spot intensities of the three samples shown in scanned images were measured through the gold circle micropatterns.

SCVme (100 μg mL^{-1}) for 30 min at 25 °C. Following washing and drying, the prepared chip was analyzed. The brighter spots indicate binding of the target proteins onto gold substrates, because reflectivity increases when binding occurs. As shown in Fig. 6(a), the brighter spots shown in samples (ii) and (iii) (compared to sample (i)) indicate the successive binding of GBP-E-SCVme and anti-SCVme antibodies onto the gold micropatterns. The brighter spots indicate the binding of target proteins onto gold substrates. Moreover, spot brightness is shown as spot intensity in Fig. 6(b). The spot intensity increased to 11.2 RU when GBP-E-SCVme was specifically bound to a gold-patterned chip showing background spot intensities of 4.6 RU, and subsequent binding of anti-SCVme to the resulting GBP-E-SCVme layer yielded a stronger spot intensity of 32.8 RU. These SPRi images show that the binding of GBP-E-SCVme, through the GBP domain, onto the gold substrate, was highly specific, and the fusion protein remained functional for further specific interaction between the SCVme domain and anti-SCVme, after immobilization onto the gold surface.

4. Conclusion

The emergence of SARS has resulted in several outbreaks worldwide. Therefore, in this study, a rapid diagnostic method of SARS was developed using a new strategy for effective immobilization of a recognition element onto an SPR gold sensor chip. The recognition element (SCVme) for detecting anti-SCVme was genetically fused to GBP. SPR analysis demonstrated that the fusion proteins were directly and simply self-immobilized onto the gold chip surface via the GBP domain which has a strong gold binding affinity, without surface modifications. The fusion protein-coated SPR chip offers a stable and specific sensing platform maintaining its anti-SCVme binding activity. Moreover, AFM analyses demonstrated specific binding of the fusion protein onto the gold surface and subsequent binding of anti-SCVme to the SCVme domain of the fusion protein layer. Using the fusion protein described here as an anchoring and recognition element, the SPR chip for rapid diagnosis of SARS infections was easily constructed and contributed to the sensitive and selective detection of anti-SCVme within 10 min. In future study, the system needs to be combined with a signal-enhancing method to obtain a more sensitive detection response. Furthermore, GBP-fusion proteins with other functional groups may open an avenue for the development of various gold substrate-based biosensor systems.

Acknowledgments

This work was supported by the Creative Research Project of Korea Food Research Institute, and supported in part by the IT Leading R&D Support Project from the MKE through IITA.

References

[1] M.A. Marra, S.J. Jones, C.R. Astell, R.A. Holt, A. Brooks-Wilson, Y.S. Butterfield, J. Khattra, J.K. Asano, S.A. Barber, S.Y. Chan, A. Cloutier, S.M. Coughlin, D. Freeman, N. Girn, O.L. Griffith, S.R. Leach, M. Mayo, H. McDonald, S.B. Montgomery, P.K. Pandoh, A.S. Petrescu, A.G. Robertson, J.E. Schein, A. Siddiqui, D.E. Smailus, J.M. Stott, G.S. Yang, F. Plummer, A. Andonov, H. Artsob, N. Bastien, K. Bernard, T.F. Booth, D. Bowness, M. Czub, M. Drebot, L. Fernando, R. Flick, M. Garbutt, M. Gray, A. Grolla, S. Jones, H. Feldmann, A. Meyers, A. Kabani, Y. Li, S. Normand, U. Stroher, G.A. Tipples, S. Tyler, R. Vogrig, D. Ward, B. Watson, R.C. Brunham, M. Krajden, M. Petric, D.M. Skowronski, C. Upton, R.L. Roper, Science 300 (2003) 1399.
[2] S.J. Lee, J.P. Park, T.J. Park, S.Y. Lee, S. Lee, J.K. Park, Anal. Chem. 77 (2005) 5755.
[3] Y.J. Tan, P.Y. Goh, B.C. Fielding, S. Shen, C.F. Chou, J.L. Fu, H.N. Leong, Y.S. Leo, E.E. Ooi, A.E. Ling, S.G. Lim, W. Hong, Clin. Diagn. Lab. Immunol. 11 (2004) 362.
[4] P.-R. Hsueh, C.-L. Kao, C.-N. Lee, L.-K. Chen, M.-S. Ho, C. Sia, X.-D. Fang, S. Lynn, T.-Y. Chang, S.-K. Liu, A.-M. Walfield, C.-Y. Wang, Emerg. Infect. Dis. 10 (2004) 1558.
[5] L.F.P. Ng, M. Wong, S. Koh, E.-E. Ooi, K.-F. Tang, H.-N. Leong, A.-E. Ling, L.V. Agathe, J. Tan, E.T. Liu, E.-C. Ren, L.-C. Ng, M.L. Hibberd, J. Clin. Microbiol. 42 (2004) 347.
[6] Y. Mizuta, T. Onodera, P. Singh, K. Matsumoto, N. Miura, K. Toko, Biosens. Bioelectron. 24 (2008) 191.
[7] Y. Sun, Y. Bai, D. Song, X. Li, L. Wang, H. Zhang, Biosens. Bioelectron. 23 (2007) 473.
[8] E. Kretschmann, H. Raether, Z. Naturforsch. 23 (1968) 2135.
[9] F. Rusmini, Z. Zhong, J. Feijen, Biomacromolecules 8 (2007) 1775.
[10] S. Brown, Nat. Biotechnol. 15 (1997) 269.
[11] M. Sarikaya, C. Tamerler, A.K. Jen, K. Schulten, F. Baneyx, Nat. Mater. 2 (2003) 577.
[12] C. Tamerler, E.E. Oren, M. Duman, E. Venkatasubramanian, M. Sarikaya, Langmuir 22 (2006) 7712.
[13] R.G. Woodbury, C. Wendin, J. Clendenning, J. Melendez, J. Elkind, D. Bartholomew, S. Brown, C.E. Furlong, Biosens. Bioelectron. 13 (1998) 1117.
[14] D.M. Hoover, J. Lubkowski, Nucleic Acids Res. 30 (2002) e43.
[15] W.P. Stemmer, A. Crameri, K.D. Ha, T.M. Brennan, H.L. Heyneker, Gene 164 (1995) 49.
[16] J. Sambrook, D.W. Russell, Molecular Cloning: A Laboratory Manual, 3rd edn., Cold Spring Harbor Laboratory Press, Cold Spring Harbor, NY, 2001.
[17] T. Kawaguchi, D.R. Shankaran, S.J. Kim, V.K. Gobi, K. Matsumoto, K. Toko, N. Miura, Talanta 72 (2007) 554.
[18] L.A. Ruiz-Taylor, T.L. Martin, F.G. Zaugg, K. Witte, P. Indermuhle, S. Nock, P. Wagner, Proc. Natl. Acad. Sci. U.S.A. 98 (2001) 852.
[19] M. Ormo, A.B. Cubitt, K. Kallio, L.A. Gross, R.Y. Tsien, S.J. Remington, Science 273 (1996) 1392.
[20] J. Lahiri, L. Isaacs, J. Tien, G.M. Whitesides, Anal. Chem. 71 (1999) 777.
[21] Subramanian, J. Irudayaraj, T. Ryan, Sens. Actuators B: Chem. 114 (1) (2006) 192–198.
[22] K.C. Grabar, R.G. Freeman, M.B. Hommer, M.J. Natan, Anal. Chem. 67 (1995) 735.
[23] J. Schmitt, P. Machtle, D. Eck, H. Mohwald, C.A. Helm, Langmuir 15 (1999) 3256.
[24] S. Ko, S.A. Grant, Biosens. Bioelectron. 21 (2006) 1283.
[25] S. Ko, B. Kim, S.-S. Jo, S.Y. Oh, J.-K. Park, Biosens. Bioelectron. 23 (2007) 51.
[26] S.V. Kolotilov, P.N. Boltovets, B.A. Snopok, V.V. Pavlishchuk, Theor. Exp. Chem. 42 (2006) 211.
[27] P.B. Richard, E. Lindner, Pure Appl. Chem. 66 (1994) 2527.
[28] R. Ekins, P. Edwards, Clin. Chem. 43 (1997) 1824.
[29] Y. Li, A.W. Wark, H.J. Lee, R.M. Corn, Anal. Chem. 78 (2006) 3158.
[30] D. Peelen, V. Kodoyianni, J. Lee, T. Zheng, M.R. Shortreed, L.M. Smith, J. Proteome Res. 5 (2006) 1580.